Pathophysiological Characteristics of Melanoma In-Transit Metastasis in a Lymphedema Mouse Model

Kohei Oashi[1], Hiroshi Furukawa[1], Hiroshi Nishihara[2], Michitaka Ozaki[3], Akihiko Oyama[1], Emi Funayama[1], Toshihiko Hayashi[1], Yuji Kuge[4] and Yuhei Yamamoto[1]

In-transit metastasis (ITM) is a unique manifestation of intralymphatic tumor dissemination, characterized by the presence of melanoma cells between the primary lesion and the draining regional lymph node basin that is clinically associated with poor prognosis. In this study, we aimed to establish an experimental animal model of melanoma ITM, as research progress in this field has been hampered by a lack of suitable experimental models. We reproduced melanoma ITM in a mouse hind limb by transplanting melanoma cells into the footpad of a mouse with lymphedema (LE). The tumor cells at the ITM site were highly proliferative, and mice with ITMs were more likely than control mice to develop distant lymph node and lung metastases. Peritumoral lymphatic vessels and tumor-associated blood vessels were increased in the primary tumor site of the LE mice. Our established ITM melanoma mouse model enabled us to clarify the molecular determinants and pathophysiology of ITM. This ITM model is also comparable to the unfavorable clinical behavior of melanoma ITM in humans and, moreover, underlined the importance of lymphangiogenic factors in the tumor dissemination through the lymphatic system.

Journal of Investigative Dermatology (2013) **133,** 537–544; doi:10.1038/jid.2012.274; published online 6 September 2012

INTRODUCTION

Cutaneous melanoma is one of the most aggressive solid tumors, and its incidence and mortality rates are increasing in most countries (Marks, 2000). The aggressiveness of melanoma is characterized by its high metastatic ability and resistance to chemotherapy (Satyamoorthy and Herlyn, 2002; Soengas and Lowe, 2003; Postovit *et al.*, 2006; Gajewski, 2007). Cutaneous melanoma metastasizes frequently via lymphatic systems, which is one of the major prognostic factors for tumor recurrence and survival (Balch *et al.*, 2001). Once the melanoma has spread to the lymphatic systems, only 40–50% of these patients survive for 5 years or more (Tsutsumida *et al.*, 2005). In-transit metastasis (ITM) is a unique pattern of intralymphatic metastasis and is associated with poor prognosis (Pawlik *et al.*, 2005a).

Traditionally, ITM has been regarded as a recurrent loco-regional disease found in the dermis or subcutaneous tissue between the primary melanoma and the regional lymph node basin. This pattern of metastasis has a reported incidence of 5–10%, but is associated with significant morbidity, and may be a source of eventual distant metastasis (Gershenwald and Fidler, 2002; Pawlik *et al.*, 2005a, b). Eighty-six percent of patients have been found to progress to systemic disease ranging from 2 to 244 months (median 16 months) following the development of ITM. The overall 5-year survival and the median survival, from the time of ITM diagnosis, have been reported as 12% and 19 months, respectively (Wong *et al.*, 1990).

The molecular determinants and pathophysiology of ITM are still poorly understood; one of the reasons seems to be a lack of suitable experimental animal models. In this study, we aimed to reproduce ITM of melanoma to clarify the pathophysiology of ITM using mice models. ITM is known to be promoted by disrupted lymph flow resulting from regional lymph node basin intervention (Cascinelli *et al.*, 1986; Calabro *et al.*, 1989; Wong *et al.*, 1990; Zogakis *et al.*,

[1]*Department of Plastic and Reconstructive Surgery, Graduate School of Medicine, University of Hokkaido at Sapporo (UHS), Sapporo, Japan;* [2]*Laboratory of Translational Pathology, Hokkaido University Graduate School of Medicine, Sapporo, Japan;* [3]*Department of Molecular Surgery, Hokkaido University School of Medicine, Sapporo, Japan and* [4]*Department of Tracer Kinetics and Bioanalysis, Hokkaido University Graduate School of Medicine, Sapporo, Japan*

This work was presented in part at the 19th and 20th Research Council Meeting of the Japan Society of Plastic Surgery in 2010 and 2011 (Yokohama, Japan, and Tokyo, Japan, respectively). This article is original and has not previously been published.

This work was done at the Department of Plastic and Reconstructive Surgery, Graduate School of Medicine, University of Hokkaido at Sapporo (UHS), Sapporo, Japan.

Correspondence: Kohei Oashi, Department of Plastic and Reconstructive Surgery, Graduate School of Medicine, University of Hokkaido at Sapporo (UHS), Kita-15 Nishi-7, Kita-Ku, Sapporo, Hokkaido 060-8638, Japan. E-mail: ko03252000@yahoo.co.jp

Abbreviations: BVA, blood vessel area; FP, footpad; IR (−), surgery without preoperative irradiation; ITM, in-transit metastasis; LE, lymphedema; luc, luciferase; LVA, lymphatic vessel area; LYVE-1, lymphatic vessel endothelial hyaluronan receptor-1; VEGF-C, vascular endothelial growth factor C

Received 21 February 2012; revised 28 May 2012; accepted 9 July 2012; published online 6 September 2012

2001; Pawlik *et al.*, 2005b); hence, we hypothesized that ITM could be reproduced when melanoma was transplanted to the hind limb of a mouse with lymphedema (LE; Oashi *et al.*, 2011).

RESULTS

LE mice developed ITM of melanoma

To create ITM of melanoma, we developed a new experimental animal model of acquired LE in the mouse hind limb in animals with LE (see Figure 1; Oashi *et al.*, 2011). Firefly luciferase (luc)–expressing melanoma cells (B16-F10-luc2; see Figure 2a) were transplanted to the LE hind limbs of mice with LE.

At 24 days after tumor transplantation, two out of five LE mice developed ITM in their LE hind limbs (see Figure 2b and c), whereas non-LE mice developed no ITM. So far, we have performed the same procedure in an additional eight LE mice, and all of these mice successfully developed ITM (data not shown).

High expression of the proliferation marker Ki-67 in ITM

A schematic representation of the experimental groups is shown in Figure 3a. The percentage of Ki-67-positive tumor cells was significantly higher in the ITM of LE mice (LE-ITM) compared with either the tumor in the footpad (FP) of non-LE mice (non-LE-FP) or LE mice (LE-FP; $P<0.05$), which indicates the high proliferative activity of LE-ITM (see Figure 3b). There was no significant difference in the expression level of Ki-67 between LE-FP and non-LE-FP.

Quantification of vessel area in tumor sections

The tumors were harvested and immunostained using anti-CD31 antibody and anti-lymphatic vessel endothelial hyaluronan receptor (LYVE)-1 antibody for the histopathological examinations (see Supplementary Materials online). The quantitative results of tumor-associated blood vessel area (BVA) are shown in Figure 3c. Tumor-associated blood vessels were defined as CD31-positive/LYVE-1-negative vessels located within the tumor mass and within an area of 100 μm from the tumor border. Tumor-associated blood vessels were homogeneously distributed throughout the

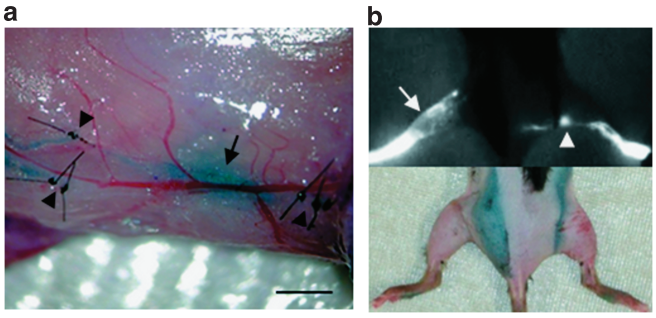

Figure 1. The lymphedema (LE) mouse. (**a**) After injecting patent blue dye into the left paw, the left side inguinal skin was circumferentially incised. The stained lymphatic vessels were carefully tied at three points with a 10-0 nylon suture, and the subiliac and popliteal lymph nodes were resected. The skin edges were sutured to underlying muscle, leaving a gap of 1–2 mm between the skin edges. Black arrow, popliteal lymph node; black arrowheads, ligations of lymphatic vessels. Bar = 1 mm. (**b**) Fluorescent lymphangiography of LE mouse 8 weeks after the lymph node resection demonstrates disappearance of major lymphatic trunks on the treated side. Normal, distinct vessel structure was replaced by a bright, punctuate fluorescence pattern over a foggy background. The bottom row represents the visual image. White arrow, treated limb; white arrowhead, popliteal lymph node of the untreated limb.

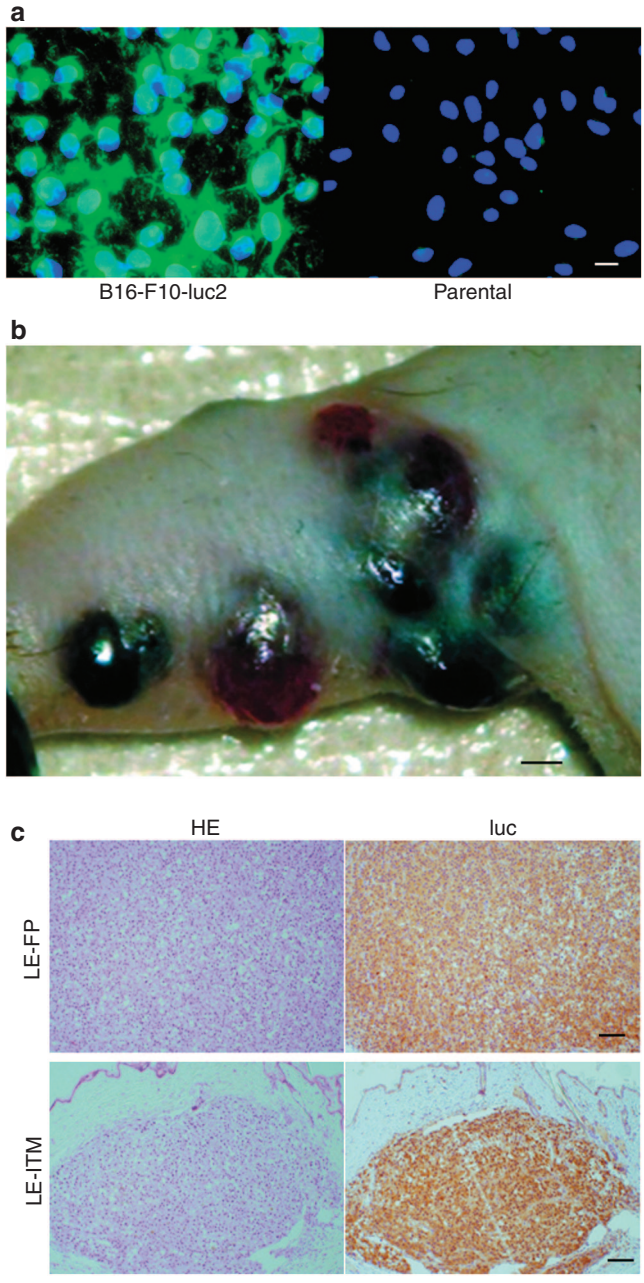

Figure 2. Luciferase (luc)-expressing B16-F10-luc2 cells cause in-transit metastasis (ITM) in the lymphedema (LE) hind limb of a mouse. (**a**) Cultured B16-F10-luc2 melanoma cells and B16-F10 parental melanoma cells were immunostained with antibodies against luc (green). Nuclear DNA was labeled with 4,6-diamidino-2-phenylindole (DAPI; blue). Bar = 100 μm. (**b**) Forty-two days after tumor transplantation into the LE hind limb of a mouse, ITMs were seen. Bar = 1 mm. (**c**) Histology of melanoma at the site of transplantation (top row) and ITM (bottom row), both of which express luc. HE, hematoxylin and eosin stains; LE-FP, LE-footpad; bar = 100 μm.

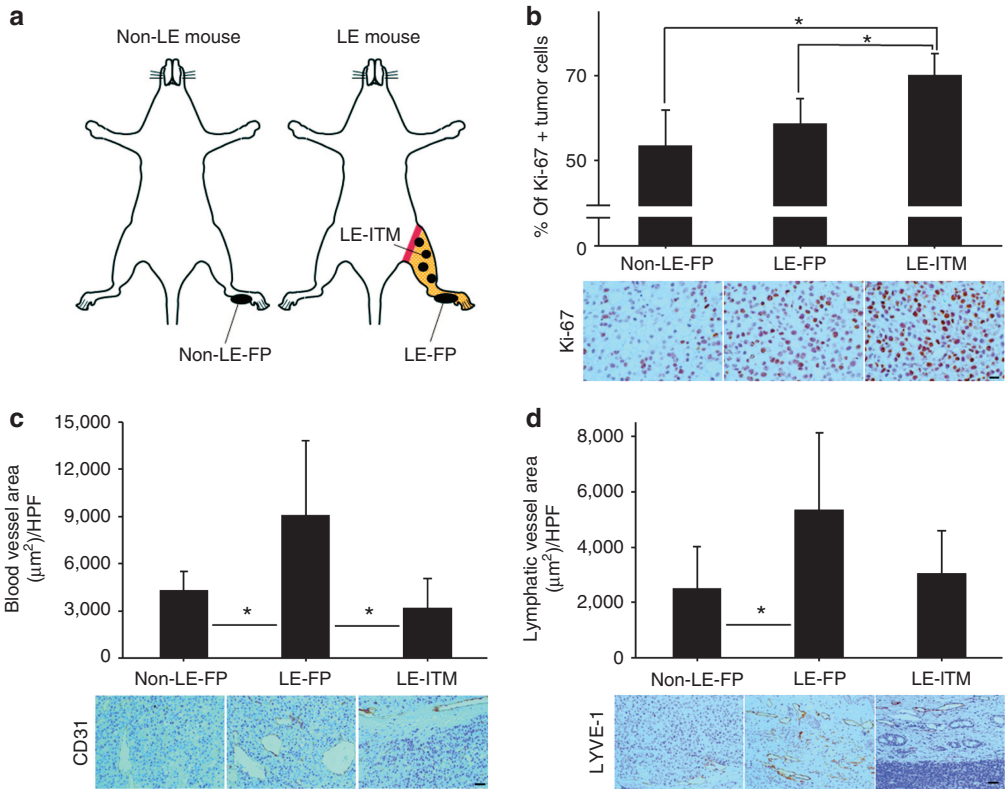

Figure 3. Characterization of in-transit melanoma. The tumors were harvested from five lymphedema (LE) mice and six non-LE mice at 24 days after transplantation for the histopathological evaluation. Three LE mice developed in-transit metastasis (ITM), which is the number of the ITM specimen. (**a**) Schematic representation of experimental groups. (**b**) The ratio of Ki-67-positive cells over the total number of tumor cells. Representative microscopic views are shown in the bottom row. Bar = 20 μm. (**c**) The area of tumor-associated CD31-positive/lymphatic vessel endothelial hyaluronan receptor (LYVE)-1-negative blood vessels. Representative microscopic views are shown in the bottom row. Bar = 50 μm. (**d**) The area of peritumoral LYVE-1-positive lymphatic vessels. Representative microscopic views are shown in the bottom row. Bar = 50 μm. HPF, high-power field; LE-FP, LE-footpad. $N = 3$–6, mean + SD, $^*P < 0.05$ after Student's *t*-test.

tumors. This finding is similar to clinical cases (Giorgadze *et al.*, 2004). BVA was larger in LE-FP compared with either non-LE-FP or LE-ITM ($P < 0.05$). There was no statistically significant difference between LE-ITM and non-LE-FP.

The quantitative results of peritumoral lymphatic vessel area (LVA) are shown in Figure 3d. Peritumoral lymphatic vessels were defined as LYVE-1-positive vessels within an area of 200 μm from the tumor border. Peritumoral lymphatic vessels were chosen for the evaluation of LVA, because intratumoral lymphatic vessels are reported to be poorly functional because of high intratumoral pressure and not required for lymphatic metastasis (Padera *et al.*, 2002; Wong *et al.*, 2005). Conversely, lymphatic vessels in the tumor periphery are functional and can drain colloids from the tumor.

In all experimental groups, peritumoral lymphatic vessels frequently had open lumina, although intratumoral lymphatic vessels frequently exhibited a thin-walled, collapsed morphology. The LVA was larger in LE-FP compared with non-LE-FP ($P < 0.05$). Although LVA in LE-FP was larger compared with LE-ITM, the difference did not reach statistical significance ($P = 0.12$). There was no statistically significant difference between LVA of LE-ITM and non-LE-FP.

In vivo bioluminescence imaging

Luc-expressing B16-F10-luc2 melanoma cells were transplanted into the left FP of both non-LE and LE mice, and serially imaged using bioluminescence imaging. To ascertain the contribution of irradiation to the metastatic pattern, the mice that underwent surgery without preoperative irradiation (IR (−) mice) were prepared. The melanoma cells were also transplanted to the left FP of IR (−) mice. Three representative mice are shown for each subline (see Figure 4a).

Seven days after tumor transplantation, signals from melanoma cells could be seen not only at the left FP but also within the left hind limb of the LE mouse, which represents pocket of ITM of melanoma. On day 14, a signal from the tumor in the left axillary lymph node could be clearly identified in the LE mouse (which was visually confirmed at necropsy). Fluorescence lymphangiography of tumors transplanted into LE mice revealed the new lymphatic flow from the left hind limb to the left axillary lymph node, which was not observed in non-LE mice (see Figure 4b). By day 20, signals from the ITM within the left hind limb of the LE mouse became remarkably enlarged. The LE mouse died because of tumor progression at around day 27.

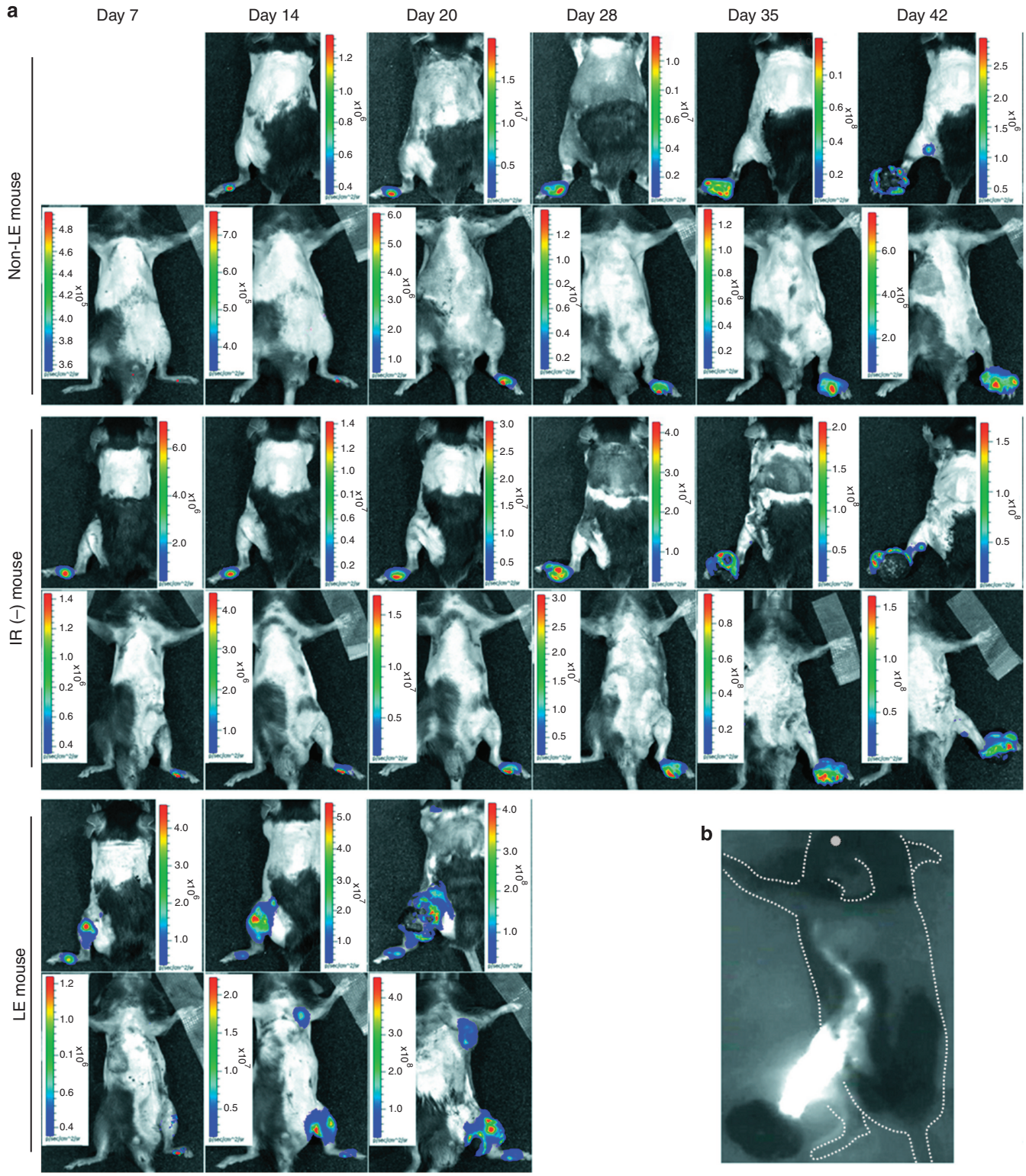

Figure 4. Bioluminescent imaging of a lymphedema (LE) and a non-LE mouse. Three mice in each group were used for the *in vivo* bioluminescence imaging, and representative images of each group are presented. (**a**) Note signal scale differences between panels. The LE mouse was dead before day 28. Top rows of the each mouse represent prone position, and bottom rows of the each mouse represent supine position. (**b**) Fluorescence lymphangiography of a tumor-transplanted LE mouse (35 days after transplantation). Dotted line represents the outline of the mouse. IR (–) mouse, mouse that underwent surgery without preoperative irradiation.

Conversely, a signal from melanoma cells was identified within the left FP of the non-LE mouse. By day 42, this signal in the left FP of the non-LE mouse had gradually enlarged. On day 42, a detectable tumor signal arose from the left popliteal lymph node in the non-LE mouse (and this was visually confirmed at necropsy). In the case of IR (−) mouse, the signal in the left FP showed similar growth pattern to the non-LE mouse, and a small signal from the ITM could be detected within the left hind limb on day 42.

LE mice developed more lung metastases

The tumor volume at the primary transplanted site 24 days after transplantation failed to show any difference between the non-LE and the LE mice (see Figure 5a).

To determine the total burden of tumor metastasized to the lung, the lungs were homogenized and total luc activity of the lung extract was examined with luminometry (see Figure 5b). The relative light units of lung extract were significantly higher in the LE mice ($P<0.05$), indicating that the LE mice had a greater burden of lung metastases. There was a robust relationship between cell number and relative light units ($r^2=0.98$; see Supplementary Figure S1a online), as well as relative light units and luc concentration ($r^2=0.99$; see Supplementary Figure S1b online).

DISCUSSION

ITM is a unique manifestation of intralymphatic tumor dissemination, characterized by the presence of melanoma in either cutaneous or subcutaneous tissue situated between the primary tumor and the draining regional lymph node basin.

In this study, we have succeeded in reproducing ITM of melanoma in the mouse hind limb using LE experimental model mice (Oashi *et al.*, 2011). To our knowledge, an experimental animal model for ITM is previously unreported. This ITM animal model enabled us to directly compare the nature of ITM with primary melanoma, using a genetically similar inbred mouse strain and melanoma cell line. To further represent clinical cases, we did not use an immunocompromised mouse metastasis model but used a syngenic mouse metastasis model, because immune responses are closely associated with the progression of melanoma (Parmiani *et al.*, 2007; Hodi *et al.*, 2010). The mice that underwent surgery without preoperative irradiation (IR (−) mice) showed mild LE and early lymphatic regeneration (data not shown). Given that it took longer time to induce ITM in IR (−) mice, the severity of lymphostasis is associated with the occurrence of ITM.

The primary tumor in the LE mice (LE-FP) had a larger area of peritumoral lymphatic vessels (see Figure 3d). Quantitative reverse-transcription PCR was performed to quantify the expression of *Vegf-C* in the tumor tissues. The expression of *Vegf-C* in the tumor tissues showed no difference between groups (data not shown). Given that the expression levels of *Vegf-C* were similar between groups, one possible reason for the enlargement of LVA in the LE-FP is the result of the morphological change in lymphatic vessels, such as abnormal dilation and curvature caused by lymphostasis (Kinmonth and Taylor, 1954; Tabibiazar *et al.*, 2006; Ogata *et al.*, 2007; Ikomi *et al.*, 2008; Stanton *et al.*, 2009). Another reason for the large LVA is that, in the LE mice, disturbed flow of interstitial fluid around the tumor resulted in the local accumulation of vascular endothelial growth factor C (VEGF-C) produced by the tumor cells, stromal cells, and lymphatic endothelial cells around the tumor in spite of the uniform level of *Vegf-C* expression. Such a local accumulation of VEGF-C around the tumor might promote lymphangiogenesis at the primary tumor site.

VEGF-C has been reported not only to promote primary tumor lymphangiogenesis but also to induce lymph node lymphangiogenesis, which might facilitate further metastatic

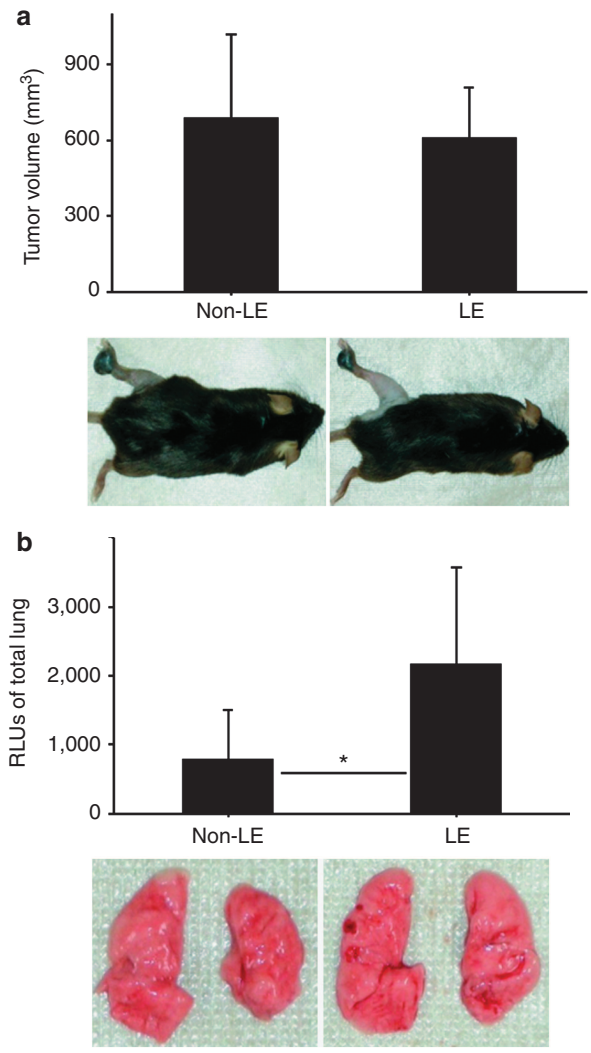

Figure 5. Tumor size and lung metastasis. The tumor volume at the primary transplanted site and the luciferase activity of the lung extract of five lymphedema (LE) mice and six non-LE mice were determined 24 days after transplantation. (**a**) The volume of the tumor was calculated with the following formula: length × width × depth/2. Representative macroscopic views are shown in the bottom row. (**b**) Lungs were excised and homogenized and total luciferase activity was determined with a standard *ex vivo* luciferase assay. Representative macroscopic views are shown in the bottom row. No black nodule (lung metastasis of melanoma cells) was observed visually. RLUs, relative light units. $N=5$-6, mean + SD, $^*P<0.05$ after Student's *t*-test.

tumor spread throughout the lymphatic system and to distant organs (Mandriota *et al.*, 2001; Skobe *et al.*, 2001; Padera *et al.*, 2002; Krishnan *et al.*, 2003; Hirakawa *et al.*, 2007; Sleeman and Thiele, 2009; Christiansen and Detmar, 2011). It is suspected that the ability of VEGF-C to induce lymph node lymphangiogenesis promotes metastasis via distal lymph nodes, the thoracic duct, and the blood vascular system to distant organs (Hirakawa *et al.*, 2007). This model is supported by the observation in the present study that LE mice were more likely than control mice to develop distant lymph node and lung metastases.

There are three other possible reasons why LE mice had a larger burden of lung metastases, except for the lymphangiogenic factor–mediated pathway. First, significantly increased Ki-67 expression was seen in the LE-ITM (see Figure 3b). ITM has a high proliferative activity, which means that it has an aggressive biological behavior and hence a greater potential to form distant metastasis. The importance of examining tumor proliferation has been underscored by the addition of mitotic rate to the 7th edition of the American Joint Committee on Cancer melanoma-staging system (Balch *et al.*, 2009). Compared with mitotic rate, the expression level of nuclear antigen Ki-67 may be a better assessment of proliferation, as Ki-67 is expressed in mitosis as well as during the G1, S, and G2 phases of the cell cycle in proliferating cells (Gerdes *et al.*, 1983). Ki-67 expression has also been shown to have prognostic value in melanoma (Tu *et al.*, 2011) and other cancers (most notably in breast cancer; Gerdes *et al.*, 1983; Railo *et al.*, 1993; Keshgegian and Cnaan, 1995; Bettencourt *et al.*, 1996; Fitzgibbons *et al.*, 2000; Mucci *et al.*, 2000). Given that the tumor cells and the animals used in this study were genetically identical, high expression of Ki-67 in ITM may have been caused by the environment surrounding the tumor or the selection of a highly proliferative tumor variant.

Second, large tumor-associated BVA (see Figure 3c) might increase the chance that invasive tumor cells enter the blood vascular system, which resulted in the formation of distant metastasis, with an increased numbers of disseminating tumor cells transplanted to distant organs.

The third possible reason is that tumor immunity was disturbed by removing the regional lymph node basin and following lymphostasis, which facilitated the tumor dissemination. Lymphatics are an important pathway for immune cell trafficking (e.g., lymphocytes, Langerhans cells, and macrophages), antigen delivery to the lymph node, and clearance of foreign antigens (Olszewski *et al.*, 1990). The occurrence of malignancy in the setting of LE is the suspected consequence of impaired local immune surveillance due to the disruption of trafficking of immunocompetent cells in the lymphedematous region (Ruocco *et al.*, 2002, 2007).

The LVA in LE-ITM was not as large as LE-FP. This discrepancy may be explained by the highly proliferative nature of ITM. Straume *et al.* (2003) found that decreased lymphatic vessel density was present in thicker and more proliferative tumors. The authors suggested that large and aggressive melanomas might destroy the lymphatics and thus made them less detectable by immunohistochemistry (Straume *et al.*, 2003).

In this study, we have succeeded in creating an experimental animal model of melanoma ITM. Our established ITM melanoma mouse model enabled us to clarify the molecular determinants and pathophysiology of ITM. This ITM model is also comparable to the unfavorable clinical behavior of melanoma ITM in humans and, moreover, underlined the importance of lymphangiogenic factors in the tumor dissemination through the lymphatic system.

MATERIALS AND METHODS

Animals

Male C57BL/6N mice weighing between 18 and 20 g were purchased from Sankyo Labo Service (Tokyo, Japan). All experiments were performed under general anesthesia. Anesthesia was induced and maintained by an intraperitoneal injection of pentobarbital (30 mg kg^{-1} body weight) or 2–3% (flow rate) isoflurane inhalation. Chronic LE in the hind limb of a mouse was created by radiation treatment and one operation—surgical division of the superficial and deep lymphatics as previously described (see Figure 1; Oashi *et al.*, 2011).

Four weeks after the surgery, the B16-F10-luc2 melanoma cells were transplanted to the hind limb as described in the next paragraph. All animal studies were conducted in accordance with Guidelines for the Care and Use of Laboratory Animals at the Hokkaido University. All procedures used in this study were approved by the local committee (Animal Care and Use Committee, Hokkaido University).

Cell lines

The B16-F10-luc2 cell line was purchased from Caliper Lifesciences (Hopkinton, MA). This luc-expressing cell line was stably transfected with firefly luc gene (*luc2*). The parental line B16-F10 was obtained from the ATCC (Rockville, MD), and B16-F10-luc2 was established by transducing a lentivirus containing the *luc2* gene under the control of human ubiquitin C promoter. This cell line was maintained in RPMI 1640 medium (ATCC catalog no. 30-2001) with 10% fetal bovine serum. Before tumor challenge, B16-F10-luc2 cells were grown in supplemented RPMI 1640, harvested, washed twice, and resuspended in Hanks' balanced salt solutions. Further, the cell suspension was injected into the FP at a dose of 4×10^5 in 0.05 ml of Hanks' balanced salt solution (Giavazzi and Garofalo, 2001). The tumors and the lungs were harvested at 24 days after tumor induction for the histopathological examinations and *ex vivo* luc assay.

Assessment of Ki-67 expression

The tumors were harvested from five LE mice and six non-LE mice at 24 days after transplantation for the evaluation of Ki-67 expression. Three LE mice developed ITM, which is the number of the ITM specimen. Five high-power fields ($\times 400$) of tumor areas with the highest density of positive nuclear staining were chosen from each slide. The percentage of Ki-67-positive tumor cells was then determined by relating the total number of positively stained tumor cells to the total number of tumor cells in all five fields. The mean value was calculated for each section.

Tumor blood vessel and lymphatic vessel area

The tumors were harvested from five LE mice and six non-LE mice at 24 days after transplantation for the evaluation of vessel area. Three LE mice developed ITM, which is the number of the ITM specimen. Sections were examined using an Olympus IX-61 microscope. Digital images were captured with an Olympus DP 70 digital camera and were processed with an Olympus DP Controller (all from Olympus Optical, Tokyo, Japan). The quantification of the vascular area was performed using the Image J software (NIH, Baltimore, MD). To analyze the LVA and BVA, the immunostained sections were first scanned at $\times 100$ magnifications, and the spot with the greatest vascularity within and around the tumor (hot spots) was selected for further evaluation. Tumor borders were determined on serial sections using hematoxylin and eosin stains or luc immunostaining.

The peritumoral LVAs were determined in four high-power fields ($\times 400$), and the mean area was calculated for each section. Single LYVE1-positive cells were considered to be macrophages and excluded from the analysis. The tumor-associated BVA was determined in eight high-power fields ($\times 400$) and the mean area was calculated for each section.

In vivo optical imaging

Three mice in each group were used for the *in vivo* bioluminescence imaging, and representative images of each group were presented in Figure 4. Before imaging, mice were anesthetized with 2% isoflurane, and 150 mg ml^{-1} of D-luciferin (VivoGlo Luciferin, *In Vivo* Grade, Promega, Madison, WI) in normal saline was intraperitoneally injected at a dose of 150 mg kg^{-1} body weight. The tumor site was shaved to minimize the amount of light absorbed by black fur, and imaged after 10–20 minutes. A cryogenically cooled IVIS system (Xenogen, Alameda, CA) coupled with a data acquisition PC running the LivingImage software (Xenogen) was used to detect photon emission from tumor-bearing mice (Contag *et al.*, 1997; Rehemtulla *et al.*, 2000; Craft *et al.*, 2005; Xing *et al.*, 2008).

Fluorescent lymphangiography was performed 15 minutes after injecting 2 µl of a 2-mg ml^{-1} solution of indocyanine green subcutaneously into the paws or just proximal to the tumor. The mice were then observed using the Near-infrared fluorescence camera system (Photodynamic Eye; Hamamatsu Photonics, Hamamatsu, Japan).

Quantification of lung metastasis

Twenty-four days after tumor transplantation, five LE mice and six non-LE mice were killed by overdose of diethyl ether. The entire lung was collected from each mouse, washed with phosphate-buffered saline, and frozen on dry ice in a 2-ml microtube immediately after collection and stored at −80 °C. Lung tissues were soaked in 800 µl of Luciferase Cell Culture Lysis Reagent in Luciferase Assay System (E1500, Promega) and crushed twice each at 4,000 r.p.m. for 30 seconds with a 5.5-mm-diameter stainless bead using a Micro Smash MS-100 (TOMY, Tokyo, Japan). The samples were frozen and thawed three times using alternating liquid nitrogen and a 37 °C heat block, vortexed for 15 minutes, and centrifuged for 3 minutes at 10,000*g*. The supernatant was transferred to 1.5-ml tubes. After adding another 200 µl of Luciferase Cell Culture Lysis Reagent to the pellet, vortex and centrifuge processes were repeated. The second supernatant was added to the first one, and then nearly 1 ml of total lung extract was stored at −80 °C until assayed (Manthorpe *et al.*, 1993).

Luc activity was assayed using a GloMax 20/20n Luminometer (Promega). Twenty microliters of lung extract was added to 100 µl of Luciferase Assay Reagent in Luciferase Assay System (E1500, Promega) in a luminometer tube, and sample light units were recorded by performing a 2-second measurement delay followed by a 10-second measurement read for luc activity.

The *in vitro* luc assay revealed a high correlation between the number of B16-F10-luc2 melanoma cells and the bioluminescent activity (see Supplementary Figure S1a online). The bioluminescent activity was not disturbed under existence of lung extract (see Supplementary Figure S1b online). Hence, the result of *ex vivo* luc assay was considered to represent the tumor burden of lung metastasis.

Statistical analysis

All error bars represent SD of the mean unless otherwise designated. The difference between groups was considered statistically significant when the *P*-value was lower than 0.05 after Student's *t*-test.

CONFLICT OF INTEREST

The authors state no conflict of interest.

ACKNOWLEDGMENTS

This study was funded by a grant-in-aid (10101-05-1-7312-0001) from the Ministry of Education, Culture, Sports, Science, and Technology of Japan.

SUPPLEMENTARY MATERIAL

Supplementary material is linked to the online version of the paper at http://www.nature.com/jid

REFERENCES

Balch CM, Gershenwald JE, Soong SJ *et al.* (2009) Final version of 2009 AJCC melanoma staging and classification. *J Clin Oncol* 27: 6199–206

Balch CM, Soong SJ, Gershenwald JE *et al.* (2001) Prognostic factors analysis of 17,600 melanoma patients: validation of the American Joint Committee on Cancer melanoma staging system. *J Clin Oncol* 19: 3622–34

Bettencourt MC, Bauer JJ, Sesterhenn IA *et al.* (1996) Ki-67 expression is a prognostic marker of prostate cancer recurrence after radical prostatectomy. *J Urol* 156:1064–8

Calabro A, Singletary SE, Balch CM (1989) Patterns of relapse in 1001 consecutive patients with melanoma nodal metastases. *Arch Surg* 124:1051–5

Cascinelli N, Bufalino R, Marolda R *et al.* (1986) Regional non-nodal metastases of cutaneous melanoma. *Eur J Surg Oncol* 12:175–80

Christiansen A, Detmar M (2011) Lymphangiogenesis and cancer. *Genes Cancer*, published online 3 October 2011; doi:10.1177/1947601911423028

Contag CH, Spilman SD, Contag PR *et al.* (1997) Visualizing gene expression in living mammals using a bioluminescent reporter. *Photochem Photobiol* 66:523–31

Craft N, Bruhn KW, Nguyen BD *et al.* (2005) Bioluminescent imaging of melanoma in live mice. *J Invest Dermatol* 125:159–65

Fitzgibbons PL, Page DL, Weaver D *et al.* (2000) Prognostic factors in breast cancer. College of American Pathologists Consensus Statement 1999. *Arch Pathol Lab Med* 124:966–78

Gajewski TF (2007) Failure at the effector phase: immune barriers at the level of the melanoma tumor microenvironment. *Clin Cancer Res* 13: 5256–61

Gerdes J, Schwab U, Lemke H *et al.* (1983) Production of a mouse monoclonal antibody reactive with a human nuclear antigen associated with cell proliferation. *Int J Cancer* 31:13–20

Gershenwald JE, Fidler IJ (2002) Cancer. Targeting lymphatic metastasis. *Science* 296:1811–2

Giavazzi R, Garofalo A (2001) Syngeneic murine metastasis models : b16 melanoma. *Methods Mol Med* 58:223–9

Giorgadze TA, Zhang PJ, Pasha T *et al.* (2004) Lymphatic vessel density is significantly increased in melanoma. *J Cutan Pathol* 31:672–7

Hirakawa S, Brown LF, Kodama S *et al.* (2007) VEGF-C-induced lymphangiogenesis in sentinel lymph nodes promotes tumor metastasis to distant sites. *Blood* 109:1010–7

Hodi FS, O'Day SJ, McDermott DF *et al.* (2010) Improved survival with ipilimumab in patients with metastatic melanoma. *N Engl J Med* 363: 711–23

Ikomi F, Kawai Y, Nakayama J *et al.* (2008) Critical roles of VEGF-C-VEGF receptor 3 in reconnection of the collecting lymph vessels in mice. *Microcirculation* 15:591–603

Keshgegian AA, Cnaan A (1995) Proliferation markers in breast carcinoma. Mitotic figure count, S-phase fraction, proliferating cell nuclear antigen, Ki-67 and MIB-1. *Am J Clin Pathol* 104:42–9

Kinmonth JB, Taylor GW (1954) The lymphatic circulation in lymphedema. *Ann Surg* 139:129–36

Krishnan J, Kirkin V, Steffen A *et al.* (2003) Differential *in vivo* and *in vitro* expression of vascular endothelial growth factor (VEGF)-C and VEGF-D in tumors and its relationship to lymphatic metastasis in immunocompetent rats. *Cancer Res* 63:713–22

Mandriota SJ, Jussila L, Jeltsch M *et al.* (2001) Vascular endothelial growth factor-C-mediated lymphangiogenesis promotes tumour metastasis. *EMBO J* 20:672–82

Manthorpe M, Cornefert-Jensen F, Hartikka J *et al.* (1993) Gene therapy by intramuscular injection of plasmid DNA: studies on firefly luciferase gene expression in mice. *Hum Gene Ther* 4:419–31

Marks R (2000) Epidemiology of melanoma. *Clin Exp Dermatol* 25:459–63

Mucci NR, Rubin MA, Strawderman MS *et al.* (2000) Expression of nuclear antigen Ki-67 in prostate cancer needle biopsy and radical prostatectomy specimens. *J Natl Cancer Inst* 92:1941–2

Oashi K, Furukawa H, Oyama A *et al.* (2011) A new model of acquired lymphedema in the mouse hind limb: a preliminary report of a half-year course. *Ann Plast Surg*, e-pub ahead of print 27 May 2011, doi:10.1097/SAP.0b013e31821ee3dd

Ogata F, Azuma R, Kikuchi M *et al.* (2007) Novel lymphography using indocyanine green dye for near-infrared fluorescence labeling. *Ann Plast Surg* 58:652–5

Olszewski WL, Engeset A, Romaniuk A *et al.* (1990) Immune cells in peripheral lymph and skin of patients with obstructive lymphedema. *Lymphology* 23:23–33

Padera TP, Stoll BR, So PT *et al.* (2002) Conventional and high-speed intravital multiphoton laser scanning microscopy of microvasculature, lymphatics, and leukocyte-endothelial interactions. *Mol Imaging* 1:9–15

Parmiani G, Castelli C, Santinami M *et al.* (2007) Melanoma immunology: past, present and future. *Curr Opin Oncol* 19:121–7

Pawlik TM, Ross MI, Johnson MM *et al.* (2005a) Predictors and natural history of in-transit melanoma after sentinel lymphadenectomy. *Ann Surg Oncol* 12:587–96

Pawlik TM, Ross MI, Thompson JF *et al.* (2005b) The risk of in-transit melanoma metastasis depends on tumor biology and not the surgical approach to regional lymph nodes. *J Clin Oncol* 23:4588–90

Postovit LM, Seftor EA, Seftor RE *et al.* (2006) Influence of the microenvironment on melanoma cell fate determination and phenotype. *Cancer Res* 66:7833–6

Railo M, Nordling S, von Boguslawsky K *et al.* (1993) Prognostic value of Ki-67 immunolabelling in primary operable breast cancer. *Br J Cancer* 68:579–83

Rehemtulla A, Stegman LD, Cardozo SJ *et al.* (2000) Rapid and quantitative assessment of cancer treatment response using *in vivo* bioluminescence imaging. *Neoplasia* 2:491–5

Ruocco E, Puca RV, Brunetti G *et al.* (2007) Lymphedematous areas: privileged sites for tumors, infections, and immune disorders. *Int J Dermatol* 46:662

Ruocco V, Schwartz RA, Ruocco E (2002) Lymphedema: an immunologically vulnerable site for development of neoplasms. *J Am Acad Dermatol* 47:124–7

Satyamoorthy K, Herlyn M (2002) Cellular and molecular biology of human melanoma. *Cancer Biol Ther* 1:14–7

Skobe M, Hawighorst T, Jackson DG *et al.* (2001) Induction of tumor lymphangiogenesis by VEGF-C promotes breast cancer metastasis. *Nat Med* 7:192–8

Sleeman JP, Thiele W (2009) Tumor metastasis and the lymphatic vasculature. *Int J Cancer* 125:2747–56

Soengas MS, Lowe SW (2003) Apoptosis and melanoma chemoresistance. *Oncogene* 22:3138–51

Stanton AW, Modi S, Mellor RH *et al.* (2009) Recent advances in breast cancer-related lymphedema of the arm: lymphatic pump failure and predisposing factors. *Lymphat Res Biol* 7:29–45

Straume O, Jackson DG, Akslen LA (2003) Independent prognostic impact of lymphatic vessel density and presence of low-grade lymphangiogenesis in cutaneous melanoma. *Clin Cancer Res* 9:250–6

Tabibiazar R, Cheung L, Han J *et al.* (2006) Inflammatory manifestations of experimental lymphatic insufficiency. *PLoS Med* 3:e254

Tsutsumida A, Furukawa H, Yamamoto Y *et al.* (2005) Treatment strategy for cutaneous malignant melanoma. *Int J Clin Oncol* 10:311–7

Tu TJ, Ma MW, Monni S *et al.* (2011) A high proliferative index of recurrent melanoma is associated with worse survival. *Oncology* 80:181–7

Wong JH, Cagle LA, Kopald KH *et al.* (1990) Natural history and selective management of in transit melanoma. *J Surg Oncol* 44:146–50

Wong SY, Haack H, Crowley D *et al.* (2005) Tumor-secreted vascular endothelial growth factor-C is necessary for prostate cancer lymphangiogenesis, but lymphangiogenesis is unnecessary for lymph node metastasis. *Cancer Res* 65:9789–98

Xing Y, Lu X, Pua EC *et al.* (2008) The effect of high intensity focused ultrasound treatment on metastases in a murine melanoma model. *Biochem Biophys Res Commun* 375:645–50

Zogakis TG, Bartlett DL, Libutti SK *et al.* (2001) Factors affecting survival after complete response to isolated limb perfusion in patients with in-transit melanoma. *Ann Surg Oncol* 8:771–8